A LETTERS JOURNAL EXPLORING THE FRONTIERS OF PHYSICS

OFFPRINT

Spurious causalities due to low temporal resolution: Towards detection of bidirectional coupling from time series

D. A. SMIRNOV and B. P. BEZRUCHKO

EPL, **100** (2012) 10005

epl

A Letters Journal Exploring the Frontiers of Physics

AN INVITATION TO SUBMIT YOUR WORK

www.epljournal.org

The Editorial Board invites you to submit your letters to EPL

EPL is a leading international journal publishing original, high-quality Letters in all areas of physics, ranging from condensed matter topics and interdisciplinary research to astrophysics, geophysics, plasma and fusion sciences, including those with application potential.

The high profile of the journal combined with the excellent scientific quality of the articles continue to ensure EPL is an essential resource for its worldwide audience. EPL offers authors global visibility and a great opportunity to share their work with others across the whole of the physics community.

Run by active scientists, for scientists

EPL is reviewed by scientists for scientists, to serve and support the international scientific community. The Editorial Board is a team of active research scientists with an expert understanding of the needs of both authors and researchers.

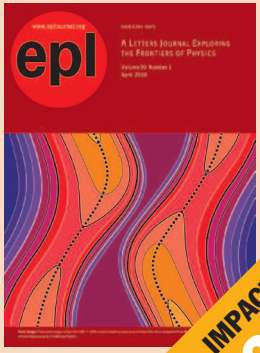

IMPACT FACTOR 2.753*

*As ranked by ISI 2010

IMPACT FACTOR
2.753*
* As listed in the ISI® 2010 Science Citation Index Journal Citation Reports

OVER
500 000
full text downloads in 2010

30 DAYS
average receipt to online publication in 2010

16 961
citations in 2010
37% increase from 2007

"We've had a very positive experience with EPL, and not only on this occasion. The fact that one can identify an appropriate editor, and the editor is an active scientist in the field, makes a huge difference."

Dr. Ivar Martinv
Los Alamos National Laboratory, USA

Six good reasons to publish with EPL

We want to work with you to help gain recognition for your high-quality work through worldwide visibility and high citations.

1. **Quality** – The 40+ Co-Editors, who are experts in their fields, oversee the entire peer-review process, from selection of the referees to making all final acceptance decisions
2. **Impact Factor** – The 2010 Impact Factor is 2.753; your work will be in the right place to be cited by your peers
3. **Speed of processing** – We aim to provide you with a quick and efficient service; the median time from acceptance to online publication is 30 days
4. **High visibility** – All articles are free to read for 30 days from online publication date
5. **International reach** – Over 2,000 institutions have access to EPL, enabling your work to be read by your peers in 100 countries
6. **Open Access** – Articles are offered open access for a one-off author payment

Details on preparing, submitting and tracking the progress of your manuscript from submission to acceptance are available on the EPL submission website **www.epletters.net**.

If you would like further information about our author service or EPL in general, please visit **www.epljournal.org** or e-mail us at **info@epljournal.org**.

EPL is published in partnership with:

European Physical Society | Società Italiana di Fisica | EDP Sciences | IOP Publishing

A Letters Journal Exploring the Frontiers of Physics

October 2012

EPL, **100** (2012) 10005
doi: 10.1209/0295-5075/100/10005

www.epljournal.org

Spurious causalities due to low temporal resolution: Towards detection of bidirectional coupling from time series

D. A. Smirnov and B. P. Bezruchko

Saratov Branch of V.A. Kotel'nikov Institute of RadioEngineering and Electronics of the Russian Academy of Sciences - 38 Zelyonaya St., Saratov 410019, Russia

received 31 May 2012; accepted in final form 13 September 2012
published online 16 October 2012

PACS 05.45.Tp – Time series analysis
PACS 05.45.Xt – Synchronization; coupled oscillators
PACS 02.50.Sk – Multivariate analysis

Abstract – The detection of causal influences is a topical problem in time series analysis. A traditional approach is based on Granger causality and increasingly often used in very diverse fields. However, a principal possibility of spurious detection of a bidirectional coupling due to low sampling rate, noted by statisticians and econometricians, remains overlooked in physical research. With models widely used in physics, including linear oscillators and nonlinear chaotic maps, we show that spurious coupling characteristics can be rather large and one may even incorrectly identify directionality of a unidirectional coupling if a sampling interval is not small enough. To avoid erroneous conclusions, we suggest a practical test to distinguish between uni- and bi-directional couplings and illustrate it with mathematical systems and climatic data.

Introduction. – The problem of detecting directional couplings (causal influences) between complex systems from time series attracts increasing attention [1–5] in various fields of physical research, including geophysics [6], biophysics [7,8], electronics [9], and communication [10]. Particularly, it is often fundamentally important to determine whether coupling between two systems is uni- or bi-directional [6,8,11]. The concept of Granger causality originating from econometrical studies [12] has appeared fruitful to address such problems and, thus, it becomes popular in physical research as well, *e.g.*, [1,5–7].

One says that a system X "Granger causes" Y if a knowledge of the past of X improves predictions of Y as compared to self-predictions. A nonzero prediction improvement (PI) in a certain direction is associated with an influence in that direction, so that nonzero PIs in both directions are interpreted as a sign of a bidirectional coupling (BC). The predictions are one step ahead, where the step is a sampling interval Δt determined by an observation procedure, *e.g.*, a given sampling frequency of an analogue-to-digit converter or usage of monthly values of climatic indices. At that, it is overlooked or underestimated in physical research that the PIs may vary with Δt in a rather nontrivial manner. Indeed, in the mathematical and econometrical literature it was indicated [13,14] that, if Δt is not small enough, PIs are typically nonzero *in both directions* even for *unidirectionally coupled* systems. This important circumstance has not yet been appreciated by physicists. It was described mostly in an abstract mathematical setting [13] and applied to evidence the principal existence of false conclusions [14] rather than to analyze quantitative characteristics of spurious couplings.

In this letter, we perform such a quantitative analysis with various models widely used in physical research and show that the "spurious" PIs can be rather large, depending on a sampling interval. Even more surprising, a single nonzero PI may correspond to a unidirectional coupling (UC) in an *opposite* direction. This "downsampling effect" appears ubiquitous, ranging from linear autoregressive (AR) processes to continuous-time oscillators and nonlinear chaotic maps. It takes place also if transfer entropy [2] (a widely used generalized version of Granger causality) is applied instead of PI. Taking the effect into account, we suggest a practical test to distinguish BC from UC and apply it to an analysis of coupling between large-scale climatic phenomena such as El-Niño/Southern Oscillation (ENSO) and Indian monsoon.

Granger causality. – Let $(X(t), Y(t))$ be a bivariate random process with $x_n = X(n\Delta t)$, $y_n = Y(n\Delta t)$, $n \in \mathbf{Z}$. The self-predictor of x_n given by $x_n^{ind} = E[x_n|x_{n-1}, x_{n-2}, \ldots]$, where $E[\cdot|\cdot]$ stands for a conditional expectation, gives the least (over all self-predictors) mean-squared error $\sigma^2_{x,ind} = E[(x_n - x_n^{ind})^2]$. The joint predictor $x_n^{joint} = E[x_n|x_{n-1}, y_{n-1}, x_{n-2}, y_{n-2}, \ldots]$ gives

the error $\sigma^2_{x,joint}$. The normalized PI value $G_{y\to x} = (\sigma^2_{x,ind} - \sigma^2_{x,joint})/\sigma^2_{x,ind}$ characterizes the Granger causality $Y \to X$. Everything is similar for $X \to Y$. The idea was first realized [12] in the application to stationary Gaussian processes (x_n, y_n). The latter yield to a bivariate linear AR equation

$$\begin{aligned} x_n &= \sum_{k=1}^{\infty} a_{x,k} x_{n-k} + \sum_{k=1}^{\infty} b_{x,k} y_{n-k} + \xi_n, \\ y_n &= \sum_{k=1}^{\infty} a_{y,k} y_{n-k} + \sum_{k=1}^{\infty} b_{y,k} x_{n-k} + \psi_n, \end{aligned} \tag{1}$$

where (ξ_n, ψ_n) is bivariate zero-mean Gaussian white noise with variances σ^2_ξ, σ^2_ψ and covariance $E[\xi_n \psi_n] = \gamma$. Whiteness assures that $\sigma^2_\xi = \sigma^2_{x,joint}$ and $\sigma^2_\psi = \sigma^2_{y,joint}$ [15]. Similarly, a process x_n yields to a univariate AR description, *i.e.*, the first line of eqs. (1) with all $b_{x,k} = 0$ and white noise $\xi_n^{'}$ with variance $\sigma^2_{\xi'} = \sigma^2_{x,ind}$. Now, $G_{y\to x}$ can be determined (and similarly for $G_{x\to y}$). To estimate these theoretical values from a finite time series $\{x_n, y_n\}_{n=1}^N$, one truncates all infinite sums at a certain p-th term and fits univariate and bivariate AR(p) models to the data via the ordinary least-squares technique. In the numerical simulations below, N is sufficiently large and p is selected just so big that the estimates do not change with its further rise (namely, $p = 10$ is used for uniformity). We check the significance of the PIs positivity via Fisher's F-test [16].

Equations (1) at different Δt are valid representations of the original system (X, Y). But how do $G_{y\to x}$ and $G_{x\to y}$ change with Δt? If there is no real influence $Y \to X$, one would hope to have $G_{y\to x} = 0$ (*i.e.*, all $b_{x,k} = 0$) at any Δt or, at least, $G_{y\to x} \ll 1$. However, both expectations fail and, moreover, a relative measure of the downsampling-induced "spurious" causality $r = G_{y\to x}/G_{x\to y}$ can be *arbitrarily large* as demonstrated below.

Examples with exact results. – We start with analytic consideration of three instants of a Q-order moving-average process X (a nonrecursive filter) driving a first-order AR-process Y (a recursive filter):

$$\begin{aligned} X(t) &= \Xi(t) + \sum_{k=1}^{Q} \Theta_k \Xi(t-k), \\ Y(t) &= \Psi(t) + A_y Y(t-1) + X(t-1), \end{aligned} \tag{2}$$

where Ξ and Ψ are independent zero-mean Gaussian white noises, Θ_k are parameters. We put $A_y = \sigma^2_\Psi = 0$ to get exact results and consider nonzero A_y and σ^2_Ψ afterwards. i) Specify $Q = 2$ and $\Delta t = 2$. The auto-covariance function (ACF) $\rho_X(l) = E[X(t)X(t+l)]$ takes the values $\rho_X(0) = \sigma^2_\Xi(1 + \Theta_1^2 + \Theta_2^2)$, $\rho_X(2) = \Theta_2 \sigma^2_\Xi$, and $\rho_X(l) = 0$ for $l > 2$. ACF of x_n is $\rho_{x,l} = E[x_n x_{n+l}] = \rho_X(2l)$ so that $\rho_{x,l} = 0$ for $l > 1$. The latter means that x_n is a first-order moving-average process and can be written as $x_n = \xi^*_n + \theta^* \xi^*_{n-1}$. Its parameters θ^* and $\sigma^2_{\xi^*}$ relate to ACF and can be found from $\rho_{x,1} = \theta^* \sigma^2_{\xi^*} = \rho_X(2)$ and $\rho_{x,0} = \sigma^2_{\xi^*}(1 + \theta^{*2}) = \rho_X(0)$. Under the univariate AR representation, x_n has an infinite order [15] and prediction error is $\sigma^2_{x,ind} = \sigma^2_{\xi^*}$.

Under the bivariate description, the first line in eqs. (1) involves $x_{n-k} = X(2n-2k)$ and $y_{n-k} = X(2n-2k-1)$, *i.e.*, the entire past of X up to the time $2n-2$ inclusively. Hence, $b_{x,k}$ are nonzero (!) and $\sigma^2_{x,joint}$ equals a two-steps-ahead prediction error of the original eq. (2), *i.e.*, $\sigma^2_\Xi(1 + \Theta_1^2)$. In particular, at $\Theta_1 = \Theta_2 = 1/2$ one derives $\theta^* = (3 - \sqrt{5})/2$, $\sigma^2_{\xi^*} = \sigma^2_\Xi/(3 - \sqrt{5}) \approx 1.31\sigma^2_\Xi$, $\sigma^2_{x,joint} = 1.25\sigma^2_\Xi$ and $G_{y\to x} \approx (1.31 - 1.25)\sigma^2_\Xi/(1.31\sigma^2_\Xi) \approx 0.045$. Thus, the *exact* value of "spurious" PI in the $Y \to X$ direction is positive. Similar considerations give $G_{x\to y} = (1.31 - 1.0)\sigma^2_\Xi/(1.31\sigma^2_\Xi) \approx 0.24$, *i.e.*, a big enough ratio $r \approx 0.19$.

ii) To evidence greater r, consider $Q = 3$ and $\Delta t = 2$. Start with $\Theta_1 = \Theta_2 = 0$. Then, $\rho_X(l) = 0$ for $l = 2$ and all $l > 3$ making x_n a white noise, so that $\sigma^2_{x,ind} = E[x_n^2] = \sigma^2_\Xi(1 + \Theta_3^2)$. The first line in eqs. (1) involves a term with $y_{n-1} = X(2n-3)$ which dominates over all others if $|\Theta_3|$ is small enough (*e.g.*, $\Theta_3^2 < 0.1$), giving $\sigma^2_{x,joint} \approx \sigma^2_\Xi$ and $G_{y\to x} \approx \Theta_3^2$. Similarly, $\sigma^2_{y,ind} = \sigma^2_\Xi(1 + \Theta_3^2)$ and the second line in eqs. (1) involves $x_{n-2} = Y(2n-3)$ giving $\sigma^2_{y,joint} \approx \sigma^2_\Xi$ and $r = 1$. Thus, PIs in both directions are *the same* despite a UC in the original system.

iii) To evidence infinite r, specify $Q = 4$ and $\Delta t = 3$. At $\Theta_1 = \Theta_2 = \Theta_3 = 0$, one gets $\sigma^2_{x,ind} = \sigma^2_\Xi(1 + \Theta_4^2)$, $\sigma^2_{x,joint} = \sigma^2_\Xi$, and $G_{y\to x} = \Theta_4^2/(1 + \Theta_4^2)$. If $|\Theta_4| \gg 1$, $G_{y\to x}$ even approaches unity, *i.e.*, a *maximal theoretically possible* value. For the opposite direction, $\sigma^2_{y,ind} = \sigma^2_{y,joint} = \sigma^2_\Xi(1 + \Theta_4^2)$ and, hence, $G_{x\to y} = 0$. Thus, the UC $X \to Y$ exhibits the *opposite* configuration of PIs after the downsampling: $G_{x\to y} = 0$, $G_{y\to x} > 0$, $r = \infty$.

Numerical estimations evidence that r and $G_{y\to x}$ remain positive and decrease gradually when $|A_Y|, \sigma^2_\Psi$, and $|\Theta_k|$ increase considerably, *e.g.*, up to 1 (not shown).

Coupled oscillators. – To give a vivid and general explanation of the downsampling effect, consider paradigmatic systems of stochastic linear dissipative oscillators. In discrete time, they read [17]

$$\begin{aligned} X(t) &= \sum_{k=1}^{2} A_{X,k} X(t-k) + B_X Y(t-1) + \Xi(t), \\ Y(t) &= \sum_{k=1}^{2} A_{Y,k} Y(t-k) + B_Y X(t-1) + \Psi(t), \end{aligned} \tag{3}$$

where Ξ and Ψ are as above, B_X and B_Y are coupling coefficients. An individual oscillation period T_x and relaxation time τ_x are given by $A_{X,1} = 2\cos(2\pi/T_x)\exp(-1/\tau_x)$, $A_{X,2} = -\exp(-2/\tau_x)$ and similarly for T_y and τ_y.

Start with moderate values of the oscillation periods and relaxation times $T_x = T_y = 5$, $\tau_x = \tau_y = 4$, noise variances $\sigma^2_\Xi = \sigma^2_\Psi = 1$, and UC $X \to Y$ provided by $B_X = 0$ and $B_Y = 0.3$. PIs estimated from long time series (to suppress statistical fluctuations) at different Δt are shown in fig. 1(a)–(c) (circles). UC is reflected correctly at $\Delta t = 1$: $G_{y\to x} = 0$, $G_{x\to y} > 0$, $\gamma = 0$. At greater Δt, nonzero γ and "spurious" $G_{y\to x}$ are observed. $G_{y\to x}$ is maximal at $\Delta t = 3$ ($r = 0.08$) and its positivity is highly significant (at the level of 10^{-12}). For $\Delta t \to \infty$, one gets $G_{y\to x} = G_{x\to y} = 0$,

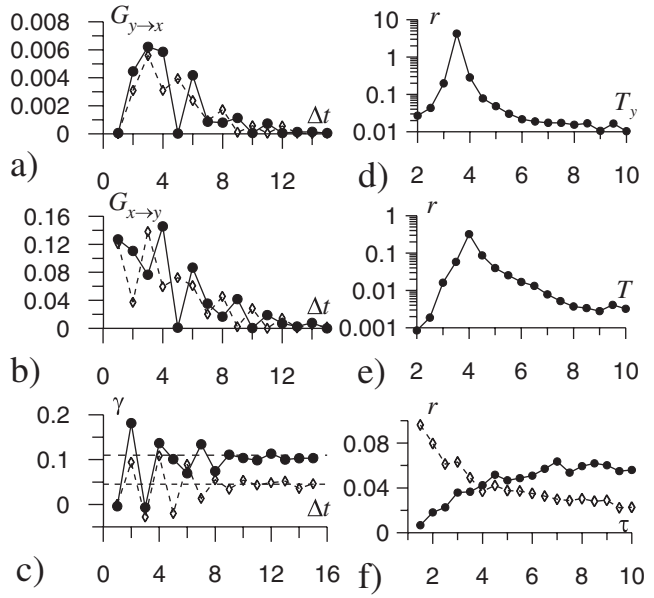

Fig. 1: PIs, γ, and r estimated from time series ($N=10^5$) of the oscillators (3) with UC $X\to Y$. (a)–(c) PIs and γ *vs.* Δt for $T_x=T_y=5$ (circles) and $T_x=T_y=4.4$ (rhombs); the horizontal dashed lines show $E[X(t)Y(t)]$. (d)–(f) The ratio r at $\Delta t=2$ *vs.* T_y at fixed $T_x=5$, *vs.* $T=T_x=T_y$, *vs.* $\tau=\tau_x$ at fixed $\tau_y=4$ (circles) and $\tau=\tau_y$ at fixed $\tau_x=4$ (rhombs).

$\gamma=E[X(t)Y(t)]$ because (x_n,y_n) turns into a white noise, see, *e.g.*, $\Delta t=15$ in fig. 1(a)–(c).

For a useful interpretation of the downsampling-induced nonzero $G_{y\to x}$, note that $X(t)$ is a second-order Markovian process, so that the vector $(X(t),X(t-1))$ contains complete information about a distribution of $X(t+l)$ for any $l>0$: $g(X(t+l)|X(t),X(t-1))=g(X(t+l)|X(t),\,Y(t),\,X(t-1),\,Y(t-1),\,X(t-2),\,Y(t-2),\ldots)$, where $g(\cdot|\cdot)$ is a conditional probability density. In terms of state space models, $(X(t),X(t-1))$ determines the state of X at time t. At $\Delta t>1$, a forecast of X based on $\{X(t),X(t-\Delta t),\ldots\}$ is not the best possible since $X(t-1)$ cannot be precisely restored from the downsampled X-data. Some predictive information may still be restored from Y due to the correlation between $X(t-1)$ and Y, allowing a nonzero $G_{y\to x}$. Thus, the rationale of the "spurious causality" is an incomplete information about a driver state in its downsampled data. A further illustration is a "stroboscopic effect" at $\Delta t=5$ in fig. 1(a), (b) when both PIs are small ($G_{y\to x}=2\cdot10^{-5}$, not significant at 0.05; $G_{x\to y}=0.001$, highly significant). The reason for this is that at $\Delta t=T_x=T_y$ the oscillators are almost first-order AR processes, *e.g.*, $a_{x,1}\approx0.29$ and other $|a_{x,k}|<0.002$ in our example. A nonzero PI in the direction of a first-order AR driver is impossible since its state is a scalar and *completely* specified by observations at any Δt. For $T_x=T_y=4.4$, PIs at $\Delta t=5$ become much larger (fig. 1(a), (b), rhombs).

Positive $G_{y\to x}$ and r are observed in wide ranges of parameters values: in fig. 1(d)–(f) one of the parameters changes while the others are fixed at their starting values. At $T_y=3.5$, r is even greater than 1 (fig. 1(d)). Note that r is so large for nonidentical oscillators, while for identical ones $r<1$ (fig. 1(e)), which seems typical. Figure 1(f) shows that r depends on the two relaxation times in different ways: it rises with τ_x and falls down with τ_y, the latter seems due to worse restoration of information about $X(t-1)$ from Y-data. Hence, a strong downsampling-induced $G_{y\to x}$ should be observed if the driver relaxation time is comparatively large and the response relaxation time is small. Indeed, at $\tau_x=10$, $\tau_y=1$, $\sigma_\Psi^2=0.01$, $T_x=T_y=5$, one gets large $G_{y\to x}=0.14$, while it is not greater than 0.01 for all cases shown in fig. 1(d)–(f).

As majority of models in physics "live" in continuous time, let us show the same effect for linear oscillators specified by stochastic differential equations (DEs),

$$\begin{aligned}\ddot X(t)+\alpha_x\dot X(t)+\omega_x^2X(t)&=\Xi(t),\\ \ddot Y(t)+\alpha_y\dot Y(t)+\omega_y^2Y(t)&=\Psi(t)+kX(t),\end{aligned}\tag{4}$$

where Ξ and Ψ are independent Gaussian noises with $E[\Xi(t_1)\Xi(t_2)]=\sigma_\Xi^2\delta(t_1-t_2)$, $E[\Psi(t_1)\Psi(t_2)]=\sigma_\Psi^2\delta(t_1-t_2)$, $\delta(t)$ is Dirac's delta, k is the coupling coefficient, $\alpha_{x,y}$ are inversely proportional to relaxation times, $\omega_{x,y}$ control oscillation frequencies, $T_{x,y}=2\pi/\omega_{x,y}$. Derivatives are used in (4) instead of differentials for a vivid notation.

PIs in fig. 2(a)–(c) were computed from time series obtained via the forward Euler scheme at $\omega_x=\omega_y=1$, $\alpha_x=\alpha_y=0.3$, $\sigma_\Xi=\sigma_\Psi=0.3$, $k=0.3$, and integration step 0.006. The "spurious" $G_{y\to x}$ starts to significantly exceed zero at $\Delta t\approx1.08$ and reaches its maximum at $\Delta t\approx3.9$. Individual oscillation periods are about $T=6.27$ and low PIs occur at $\Delta t\approx kT/2$ where the oscillators are close to first-order AR processes, similarly to the above example. The state here is specified by $X(t),\dot X(t)$ rather than by subsequent $X(t)$ and cannot be precisely restored from X at any Δt. Thus, a principal possibility of nonzero $G_{y\to x}$ exists at any Δt. However, even if theoretically positive, $G_{y\to x}$ is rather small at small Δt so that one would need an extremely long time series to detect it with significance. The nonzero $G_{y\to x}$ remains in a wide range of the oscillators parameters (fig. 2(d)–(f)).

A widely used time-delay embedding based on the first minimum of the mutual information [18] corresponds to the above $\Delta t\approx T/4$. Hence, it may well exhibit spurious causality and should be used for coupling analysis with care and an additional testing procedure developed below.

Note on nonlinearity. – In nonlinear systems, including those with chaotic properties, we observed the same effect due to the same reasons as in the above linear examples. In particular, consider a stochastically perturbed two-dimensional quadratic map $X(t)=1+aX(t-1)-bX^2(t-2)+\Xi(t)$, where $\Xi(t)$ is a sequence of independent random variables uniformly distributed over $[-\epsilon/2,\epsilon/2]$. At $a=0.4$, $b=1$, $\epsilon=0$, the map exhibits a chaotic attractor with the largest Lyapunov exponent $\lambda\approx0.08$. Take $Y(t)=X(t-1)$ and $\Delta t=2$. We express $X(t)$ via $X(t-2)$

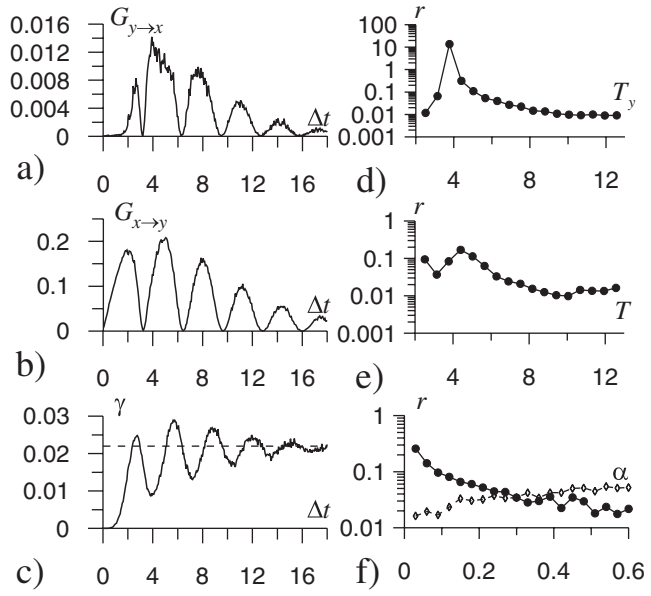

Fig. 2: PIs, γ, and r estimated from time series ($N=10^5$) of the oscillators (4). (a)–(c) PIs and γ *vs.* Δt, the horizontal dashed line shows $E[X(t)Y(t)]$. (d)–(f) The ratio r at $\Delta t=2.4$ *vs.* T_y at fixed $\omega_x=1$, *vs.* $T=T_x=T_y$, *vs.* $\alpha=\alpha_x$ at fixed $\alpha_y=0.3$ (circles) and $\alpha=\alpha_y$ at fixed $\alpha_x=0.3$ (rhombs).

and $X(t-4)$ to derive a nonlinear univariate AR model for X with an AR-order $p=2$ and a 4th-degree polynomial. It gives $\sigma^2_{x,ind}\approx\sigma^2_\Xi(1+a^2+4b^2(E[X^2])^2)$ for $\epsilon<0.1$. Similarly, a bivariate AR model gives $\sigma^2_{x,joint}\approx\sigma^2_\Xi(1+a^2)$. In particular, at $a=0.4$, $b=1$, and $\epsilon=0.1$, one gets rather large $G_{y\to x}\approx 0.6$.

If Y is also a stochastic nonlinear map driven by X, nonlinear Granger causality estimation with polynomial AR models exhibits smaller but significantly positive $G_{y\to x}$ in a wide range of parameter values, similarly to our linear examples (not shown for brevity). The effect occurs both for perturbed chaotic and regular regimes.

Spurious causality remains if transfer entropy (TE) [2,3,10] is used instead of PI. Indeed, TE is defined as the difference between Shannon entropies of the conditional distributions $g(x_n|\{x_{n-k}\})$ and $g(x_n|\{x_{n-k},y_{n-k}\})$. It represents the Kullback-Leibler divergence [2], which is nonzero as soon as $g(x_n|\{x_{n-k}\})$ and $g(x_n|\{x_{n-k},y_{n-k}\})$ are nonidentical, while PI is nonzero only if the expectations $E[x_n|\{x_{n-k}\}]$ and $E[x_n|\{x_{n-k},y_{n-k}\}]$ of those distributions do not coincide. Thus, a nonzero PI (*e.g.*, as in the above example) implies nonidentical distributions and, hence, a nonzero TE. This is even more obvious for linear systems, where TE uniquely relates to PI [5].

Test for bidirectionality. – Thus, to infer a BC, it is not enough to obtain significantly positive estimates of $G_{y\to x}$ and $G_{x\to y}$ from a time series $\{x_n,y_n\}_{n=1}^N$ at a certain Δt. One must specially test against the null hypothesis of UC. For that, we suggest to specify a class $\mathbf{M}$ of (X,Y) models with UC and an "intrinsic time step" less than Δt and search for a model capable of reproducing all appropriate properties of the observed (x_n,y_n)-data. If such a model exists, the UC hypothesis cannot be rejected.

To implement the idea for stationary Gaussian processes, consider the class $\mathbf{M}$ of discrete-time models,

$$X(t)=\sum_{k=1}^{P^*}A^*_{x,k}X(t-k\tau)+\sum_{k=1}^{S^*}B^*_{x,k}Y(t-k\tau)+\Xi^*(t),$$

$$Y(t)=\sum_{k=1}^{Q^*}A^*_{y,k}Y(t-k\tau)+\sum_{k=1}^{R^*}B^*_{y,k}X(t-k\tau)+\Psi^*(t),$$

where noise variances are $\sigma^2_{\Xi^*}$ and $\sigma^2_{\Psi^*}$, a step $\tau=\Delta t/L^*$, *i.e.*, τ is L^* times smaller than the sampling interval. Both $X\to Y$ and $Y\to X$ directions of UC can be checked in turn. For definiteness, consider testing UC $X\to Y$, *i.e.*, models with $S^*=0$. Then, $\mathbf{M}$ is specified by the quadruple (P^*,Q^*,R^*,L^*). Since all the properties of Gaussian processes are completely determined by ACFs and the cross-covariance function (CCF) [15], let us derive a distribution of sample ACF and CCF estimates for the model and, thereby, an analytic criterion for a statistical agreement between CFs of the model and sample CFs of the data.

Denote $\theta^*=(\{A^*_{x,k}\},\{A^*_{y,k}\},\{B^*_{y,k}\},\sigma^*_\Xi,\sigma^*_\Psi)$, a parameter vector of dimension $D^*=P^*+Q^*+R^*+2$. Given θ^*, ACFs and CCF of the model are found exactly from a linear set of equations obtained via multiplying model equations by $X(t-t')$ and $Y(t-t')$ in turn and taking expectations of both sides. Solving those equations for $0\leqslant t'\leqslant K\Delta t$, one gets a vector of CF values $\rho^*(\theta^*)=(\{\rho^*_X(l\Delta t)\}_{l=0}^K,\{\rho^*_Y(l\Delta t)\}_{l=0}^K,\{\rho^*_{XY}(l\Delta t)\}_{l=-K}^K)$ of dimension $D=4K+3$. Denote estimates of ρ^* from Δt-sampled model realizations $x^*_n=X(n\Delta t),y^*_n=Y(n\Delta t)$ via $\hat\rho^*$, having, *e.g.*, $\hat\rho^*_{XY}(l\Delta t)=(1/N)\sum_{n=1}^N x^*_n y^*_{n+l}$. If N is large enough, $\hat\rho^*$ is distributed according to D-dimensional Gaussian law with expectation ρ^* and covariance matrix $\mathbf{C}$. The latter is expressed via ρ^* according to Bartlett's formula, see, *e.g.*, [15]. The quantity $\chi^{*2}_D=(\hat\rho^*-\rho^*)^{\mathrm{T}}\mathbf{C}^{-1}(\hat\rho^*-\rho^*)$ (T means transposition) yields to χ^2 distribution with D degrees of freedom.

Now, denote $\hat\rho$ the vector of sample CFs for the observed data $\{x_n,y_n\}_{n=1}^N$ and $\hat\chi^2=(\hat\rho-\rho^*)^{\mathrm{T}}\mathbf{C}^{-1}(\hat\rho-\rho^*)$. Minimise $\hat\chi^2$ over θ^* and get the value of $\hat\chi^2_{\min}$. If the observed process belongs to $\mathbf{M}$, then $\hat\chi^2_{\min}$ yields to χ^2 distribution with $D-D^*$ degrees of freedom. Denote $(1-q)$-quantile of that distribution via χ^2_{1-q}. If $\hat\chi^2_{\min}>\chi^2_{1-q}$, the null hypothesis is rejected at the significance level q which represents the rate of false positives. Below, we use $q=0.05$.

The null hypothesis can be erroneously rejected if P^*,Q^*,R^* are not large enough or L^* is inappropriate. Hence, one should vary those values in some range (of course, prior substantial ideas about appropriate values are always desirable but rarely available) repeating the test for different P^*,Q^*,R^*,L^*. Under such multiple testing, the hypothesis of UC is to be rejected if it is rejected *for all* trial P^*,Q^*,R^*,L^*, *i.e.*, if no UC model

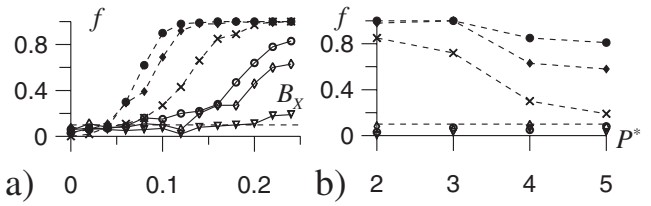

Fig. 3: Rejection rate *vs.* parameters: (a) crosses, filled rhombs, filled circles correspond to $N = 1000$, 2000, 3000 at $P^* = Q^* = 2$, $R^* = 1$; open triangles, rhombs, circles: the same at $P^* = Q^* = R^* = 5$. (b) For $P^* = Q^*$ and $R^* = 1$ crosses, filled rhombs, filled circles (dashed lines): the same at $B_X = 0.16$; open triangles, rhombs, and circles (no lines): the same at $B_X = 0$. The horizontal dashed lines show the allowable false-positives rate, exceeding $q = 0.05$ due to finite ensemble size.

consistent with the data is found. If one checks the values up to $P^*_{\max}, Q^*_{\max}, R^*_{\max}, L^*_{\max}$ (denote it $\mathbf{M}_{\max}$) and all trial L^* are dividers of $L^*_{\max}$, then the largest class $\mathbf{M}_{\max}$ contains all the other trial classes and, therefore, total significance level of the multiple test equals a separate q-level for $\mathbf{M}_{\max}$. Power (the rate of true positives) of the multiple test also coincides with that for $\mathbf{M}_{\max}$. If several aliquant L^* are considered, the total significance level is at least not greater than q. Below, we check only the rates of false and true positives for each $\mathbf{M}$ separately. We take $K = 20$ to cover nonzero values of CFs and set all nondiagonal values of $\mathbf{C}$ equal to zero to simplify the minimization of $\hat{\chi}^2(\theta^*)$. The latter may lead only to underestimation of $\hat{\chi}^2_{\min}$, so that the false-positives rate does not increase as required.

For the oscillators (3) with $B_Y = 0.3$ and various B_X we generate ensembles of 100 time series of a fixed length $N = 1000$, 2000, 3000 at fixed $\Delta t = 2$. $B_X = 0$ corresponds to UC $X \to Y$ and still nonzero $G_{y\to x}$ (fig. 1(a)). A time series estimate of $G_{y\to x}$ is significantly positive (at the level of 0.05 via F-test) with a probability of 0.22 at $N = 1000$, 0.53 at $N = 2000$, and 0.68 at $N = 3000$. Thus, a spurious BC detection is quite probable. The test against the null hypothesis of UC $X \to Y$ is performed for each simulated time series with $L^* = 2$ and P^*, Q^*, R^* ranging from 1 to 5. We calculate the rejection rate f, which is the rate of false positives at $B_X = 0$ and then must not exceed the claimed $q = 0.05$. This is the case at all P^*, Q^*, R^* in fig. 3(a), (b). At $B_X > 0$, f is the rate of true positives which rises with B_X and achieves rather large values if P^*, Q^*, R^* are not too large (fig. 3(a)). f decreases with decreasing N and rising P^*, Q^*, R^* (fig. 3(b)) as expected, since a wider model class is more probable to contain models with CFs close to the observed ones within estimation errors which are greater for smaller N. All the results are very similar for $\Delta t = 3$ and $\Delta t = 4$ at $L^* = \Delta t$ (not shown). Thus, the test works properly.

One can use $\mathbf{M}$ consisting of linear stochastic DEs with the only difference that ρ^* is found via solving the corresponding ordinary DEs[1]. The test can be implemented for nonlinear systems, but with greater difficulties. First, a global search for a UC model in a richer class of nonlinear equations is a harder computational problem. Second, one should require a model to reproduce various statistical moments of the data, while exact formulas for the model moments are rarely available so that their simulation-based estimates are to be used. Up to now, we have realized such a nonlinear test only for quadratic maps where some moments are expressed exactly via model coefficients.

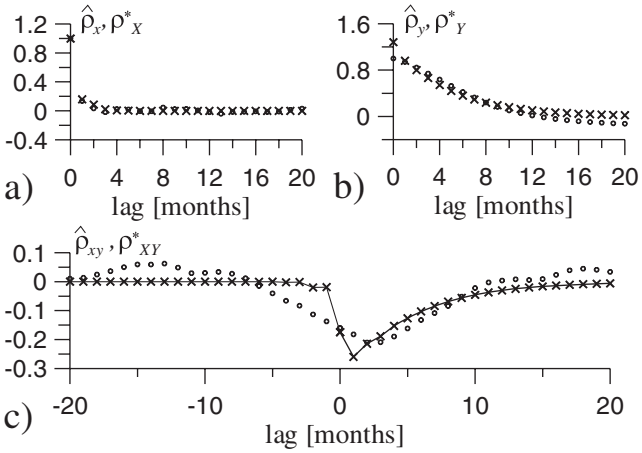

Fig. 4: Covariance functions of climatic data (circles) and a UC model with $P^* = Q^* = 3$, $R^* = 1$, $L^* = 2$ (crosses).

Climatic example. – ENSO and Indian monsoon are large-scale phenomena in Asian-Pacific region, which have even a global impact [19]. Positive PIs in both directions were revealed [20] from monthly values of x_n (monsoon index [21] with removed annual cycle) and y_n (ENSO index Niño-3 [22]) over the period 1871–2006, *i.e.*, $\Delta t = 1$ month, $N = 1632$. Namely, $G_{y\to x} = 0.020$ and $G_{x\to y} = 0.017$ (significant at the level of 0.001) were obtained with linear AR models, while including nonlinear model terms did not give any changes. Thus, a BC was inferred and possible mechanisms underlying influences in both directions were discussed. The monsoon-to-ENSO effect appeared physically less clear for climatologists. It was suggested to be due to an influence of the monsoon system on the trade winds in the Pacific and, hence, on the ENSO dynamics [20], but a further check is desirable. Moreover, we have demonstrated an example (3) with a UC and similar PIs, especially when relaxation times differ for the two processes. And ACF of the monsoon index decays faster than that of the ENSO index (fig. 4(a) (b)), giving another motivation to test against a UC.

Since the observed indices represent the total monthly value of all-India rainfall and the mean monthly value of the sea surface temperature, one deals here with physical quantities averaged over Δt corresponding to $x_n = (1/\Delta t)\sum_{i=1}^{\Delta t} X((n-1)\Delta t + i)$ in the example (3).

[1]Testing against UC was done in ref. [14] for two concrete linear DEs. Those approaches require exact formulas for a Δt-sampled representation of an original DE and, thus, are not readily applicable in practice to a general linear DE and, especially, to a discrete-time system. Moreover, they just compare UC and BC models but do not check validity of a UC model, that may distort the conclusions.

Such a combination of averaging and downsampling induces spurious causalities which are very close to those for "pure" downsampling (not shown). In the above test, averaging is straightforwardly taken into account by computing ρ^* as CFs of Δt-averaged model variables X, Y.

Both "ENSO $\rightarrow$ monsoon" and "monsoon $\rightarrow$ ENSO" hypotheses were checked with the suggested test at $L^* = 2$ (a model time step of two weeks), $L^* = 3$ (a decade), and $L^* = 4$ (a week). These time scales are shorter than a month, that seems appropriate for atmospheric processes. P^*, Q^*, R^*, S^* were varied in the range from 1 to 5. Both UC hypotheses were rejected at $q = 0.05$ in all cases. The best agreement between model and observed CFs was achieved at $L^* = 2, P^* = Q^* = 3, R^* = 1$, *i.e.*, monsoon-to-ENSO driving (fig. 4). ACFs of that model (crosses) are reasonably close to those of the data in contrast to CCFs (fig. 4(c)). Namely, the CCF of the data exhibits a maximum absolute value at a time lag of two months (monsoon "leads") while its values at small negative lags are also big enough. However, any model with UC $X \rightarrow Y$ could exhibit such a slowly changing CCF only if ACF of X were not quickly decaying. Thus, it can reproduce either ACF of monsoon or CCF, but not both functions together, that reflects inadequacy of a UC model with monsoon-to-ENSO driving. The test gives a quantitative measure for that inadequacy, namely, $\hat{\chi}^2_{\min} = 144 > \chi^2_{0.95} = 95.1$. The models with the opposite UC disagree with the data even more strongly (not shown). Thus, a BC is confirmed by the suggested test, at least, for the trial range of "intrinsic" time steps from a week to a month.

Conclusion. – Our quantitative study of Granger causality characteristics shows that a sampling interval can strongly influence results of a directional coupling analysis: Large "spurious" PIs are often induced by downsampling and even a reliable determination of a UC directionality is not assured. The effect is demonstrated with various examples, including linear oscillators and nonlinear chaotic maps. It persists if transfer entropy is used instead of PI. This investigation complements mathematical discussions [13,14] by showing the importance of the effect for physical research. In particular, it suggests that even the coupling estimation based on optimized time lags [3] should be interpreted with care. We have developed a practical test for coupling bidirectionality and confirmed a BC between ENSO and Indian monsoon.

* * *

The work is supported by RFBR, RAS program, and FP Scientific brain-power of innovative Russia for 2009–2013.

REFERENCES

[1] Ancona N., Marinazzo D. and Stramaglia S., *Phys. Rev. E*, **70** (2004) 056221; Marinazzo D., Pellicoro M. and Stramaglia S., *Phys. Rev. Lett.*, **100** (2008) 144103.

[2] Schreiber T., *Phys. Rev. Lett.*, **85** (2000) 461; Staniek M. and Lehnertz K., *Phys. Rev. Lett.*, **100** (2008) 158101; Hlavackova-Schindler K. *et al.*, *Phys. Rep.*, **441** (2007) 1; Hahs D. W. and Pethel S. D., *Phys. Rev. Lett.*, **107** (2011) 128701.

[3] Vlachos I. and Kugiumtzis D., *Phys. Rev. E*, **82** (2010) 016207; Faes L., Nollo G. and Porta A., *Phys. Rev. E*, **83** (2011) 051112.

[4] Rosenblum M. G. and A. S. Pikovsky, *Phys. Rev. E*, **64** (2001) 045202(R); Smirnov D. A. and Bezruchko B. P., *Phys. Rev. E*, **68** (2003) 046209.

[5] Barnett L., Barrett A. B. and Seth A. K., *Phys. Rev. Lett.*, **103** (2009) 238701.

[6] Wang W. *et al.*, *J. Clim.*, **17** (2004) 4752; Palus M. and Novotna D., *Nonlinear Proc. Geophys.*, **13** (2006) 287; Verdes P. F., *Phys. Rev. Lett.*, **99** (2007); Smirnov D. A. and Mokhov I. I., *Phys. Rev. E*, **80** (2009) 016208.

[7] Pereda E., Quian Quiroga R. and Bhattacharya J., *Prog. Neurobiol*, **77** (2005) 1; Brea J., Russell D. F. and Neiman A. B., *Chaos*, **16** (2006) 026111; Schelter B. *et al.*, *J. Neurosci. Methods*, **152** (2006) 210; Andrzejak R. G. and Kreuz T., *EPL*, **96** (2011) 50012.

[8] Porta A. *et al.*, *Biol. Cybern.*, **81** (1999) 119; Rosenblum M. G. *et al.*, *Phys. Rev. E*, **65** (2002) 041909; Palus M. and Stefanovska A., *Phys. Rev. E*, **67** (2003) 055201(R).

[9] Bezruchko B. *et al.*, *Chaos*, **13** (2003) 179.

[10] Hung Y.-C. and Hu C.-K., *Phys. Rev. Lett.*, **101** (2008) 244102.

[11] Mokhov I. I. and Smirnov D. A., *Geophys. Res. Lett.*, **33** (2006) L0378; Smirnov D. *et al.*, *EPL*, **83** (2008) 20003.

[12] Granger C. W. J., *Econometrica*, **37** (1969) 424.

[13] Sims C. A., *Econometrica*, **39** (1971) 545; Christiano L. J. and Eichenbaum M. S., *Carnegie-Rochester Conf. Ser. Public Policy*, **26** (1987) 63; Marcellino M., *J. Bus. Econ. Stat.*, **17** (1999) 129.

[14] Renault E., Sekkat K. and Szafarz A., *J. Empir. Finance*, **5** (1998) 47; McCrorie J. R. and Chambers M. J., *J. Econom.*, **132** (2006) 311.

[15] Box G. E. P. and Jenkins G. M., *Time Series Analysis. Forecasting and Control* (Holden-Day, San Francisco) 1970.

[16] Seber G. A. F., *Linear Regression Analysis* (Wiley, New York) 1977.

[17] Timmer J., Lauk M., Pfleger W. and Deuschl G., *Biol. Cybern.*, **78** (1998) 349.

[18] Fraser A. M. and Swinney H. L., *Phys. Rev. A.*, **33** (1986) 1131.

[19] Solomon S. *et al.* (Editors), *Climate Change. 2007: The Physical Science Basis* (Cambridge University Press, Cambridge) 2007; Yamasaki K., Gozolchiani A. and Havlin S., *Phys. Rev. Lett.*, **100** (2008) 228501; Maraun D. and Kurths J., *Geophys. Res. Lett.*, **32** (2005) L15709.

[20] Mokhov I. I., Smirnov D. A. and Nakonechny P. I. *et al.*, *Geophys. Res. Lett.*, **38** (2011) L00F04.

[21] `http://climexp.knmi.nl/data/pALLIN.dat`.

[22] `http://climexp.knmi.nl/data/iersst_nino3a.dat`.